International Journal of Fracture **84:** 307–323, 1997.

Polymer reinforcements for retarding fatigue crack growth in metals

ALAN T. ZEHNDER[1], DANIEL V. SWENSON[2] and THOMAS J. PIENKOS[3]
[1]*Associate Professor, Department of Theoretical and Applied Mechanics, Cornell University, Ithaca, NY 14853, (607)255-9181, (607)255-2011 (fax), e-mail: atz2@cornell.edu*
[2]*Associate Professor, Department of Mechanical Engineering, Kansas State University, Manhattan, Kansas, 66506, (913)532-5610, e-mail: swenson@ksume.me.ksu.edu*
[3]*Undergraduate student, University of Notre Dame, South Bend, Indiana, and summer research student at Cornell University*

Received 20 May 1996; accepted in revised form 27 February 1997

Abstract. Pure rolled, annealed copper and copper-polyimide (Kapton) laminates were tested under constant amplitude cyclic loading to determine the fatigue crack growth rate. It was found that the laminated samples could sustain a much higher load for the same fatigue life, or had a longer fatigue life for the same load. This result is due to the polyimide bridging across cracks in the copper. The reduction of the crack tip stresses due to bridging is quantified by an analytical approximation and by layered finite element analyses. Despite the low elastic modulus of polyimide relative to copper, the stress reduction is significant due to the high effective stiffness of the bridging layer which results from the thinness of the adhesive layer between the copper and polyimide. When the experimental data from the laminated samples are analyzed using the results of a layered finite element analysis good correlation is obtained between the crack growth rate in pure copper and in the copper-polyimide laminates.

1. Introduction

Fatigue crack growth rates in metals can be significantly reduced by reinforcing the metal with low modulus polymer layers. This result, surprising at first, due to the low elastic modulus of polymers relative to metals, is demonstrated here experimentally and analytically. The mechanism of reinforcement and subsequent crack growth rate decrease is bridging across cracks in the metal by the polymer layers. If the polymer layers remain intact and well bonded to the metal layers, and if the adhesive layer bonding the polymer layer to the metal is thin, the polymer layer will bridge across cracks in the metal with sufficient stiffness to significantly shield the crack tip.

This effect was first observed in copper-polyimide(Kapton) flex cables (Zehnder and Ingraffea, 1995). Laminates of annealed copper strips with and without coverlayers of polyimide were tested by repeated, fully reversed bending around a mandrel. Laminates with the polyimide coverlayers had a fatigue life approximately ten times longer than the laminates without coverlayers, although both were subjected to exactly the same cyclic loading. This result was explained in terms of a crack bridging model that treated the polyimide as a spring across cracks in the copper. The model provided only an explanation of the bridging, since it contained some arbitrary assumptions about the geometry of the bridging.

The bridging effect is also observed in other material systems. For example the substantial increase in the fatigue life of ARALL, an aluminum alloy-aramid fiber laminate, relative to the corresponding monolithic aluminum alloy is due to the fibers bridging across cracks in the aluminum (Schive, 1991; Yeh, 1995). The elastic modulus of the aramid fibers in

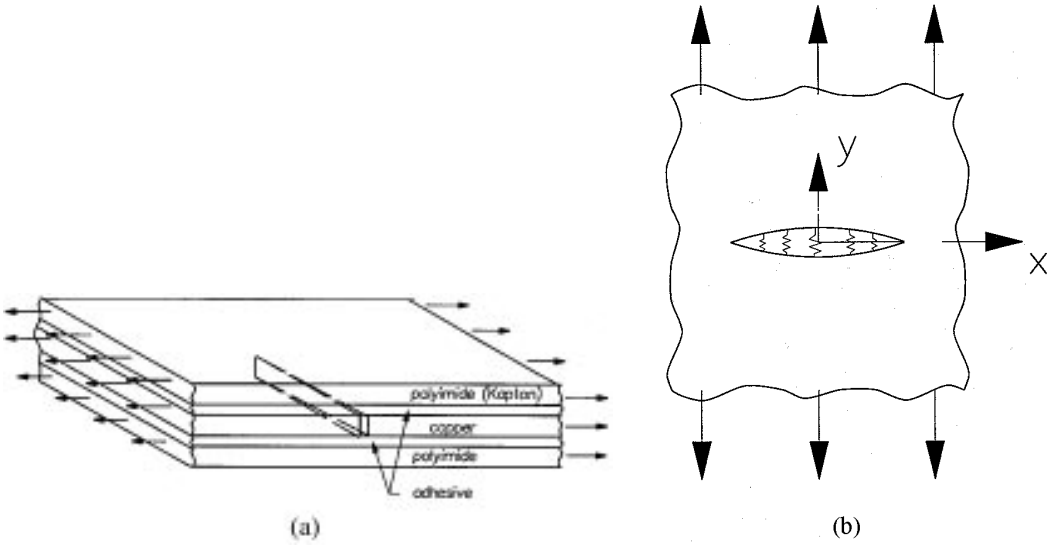

Figure 1. (a) Crack growth in copper, note that the polyimide layers remain intact. (b) Idealization of the polyimide layers bridging the crack as linear springs.

ARALL is comparable to aluminum, and thus it is not surprising that they can lend significant reinforcement to the laminate. In the case of copper-polyimide, the modulus of polyimide is just 3 percent of the modulus of copper and yet it also contributes significant shielding to the laminate.

In the experiments discussed here, center cracked sheets of pure, rolled-annealed copper, and of copper-polyimide laminates were loaded in constant amplitude cyclic tension while recording the crack length history. The data were analyzed in terms of the fatigue crack growth rate, $\mathrm{d}a/\mathrm{d}N$, vs. the cyclic stress intensity factor, ΔK_{I}. Two analyses were performed. In the first, bridging is modelled as distributed, linear springs stretching across the crack in the copper layer with a stiffness estimated using a one-dimensional shear lag analysis. The estimated stiffness was used with the results of Rose (1987) to estimate K_{I} for the laminates. In the second analysis, a layered, two dimensional finite element approach was used to accurately compute K_{I} for the laminated test specimens.

2. Analytical approximation

In the experiments, cracks in the copper layers did not penetrate the polyimide layers, that is, right up to the point of unstable crack growth, the polyimide remained intact and bridged across the crack in the copper layer, as shown in Figure 1a. Although the problem is three dimensional, because the layers are thin relative to the in-plane dimensions of the specimens, the analyses are simplified to two dimensions by modelling the bridging of the polyimide layers as linear springs acting across the crack, as shown in Figure 1b. This model captures the essence of the bridging phenomenon, while allowing us to perform the analytical calculation for the purpose of finding the scaling laws and to numerically compute the stress intensity factors without an inordinate number of degrees of freedom.

Table 1. Mechanical properties and layer thicknesses

Material	E, GPa	ν	σ_0, MPa	α,$^\circ$C^{-1}	h, μm
Copper (rolled, annealed)	124.0	0.34	180.0	17.0×10^{-6}	50.8
Polyimide (Kapton)	3.4	0.36	—	20.0×10^{-6}	50.8, 25.4
Adhesive (WA Acrylic)	1.0	0.38	—	—	25.4

The first step in the analysis is to determine the stiffness, or spring constant, of the bridging layers. This is accomplished using a shear lag model where the polyimide and copper are modelled as one-dimensional strips and the adhesive between the copper and polyimide is modelled as a distributed shear spring. The approach taken here is similar to analyses of bonded patches (Rose, 1981; Tarn and Shek, 1991).

Calculation of the effective bridging stiffness follows the familiar shear lag approach, using the geometry shown in Figure 2. In this model it is assumed that the crack penetrates the copper and adhesive layers, and that the adhesive layer carries no tensile stresses, only interlaminar shear. The mechanical properties of the layers are given in Table 1. By considering the free body diagram of the copper and of the polyimide layers separately, the following equilibrium equations are obtained:

$$h_C \sigma'_C(y) - 2\tau(y) = 0,$$
$$h_P \sigma'_P(y) + \tau(y) = 0,$$

where the subscripts C and P refer to the copper and polyimide layers respectively, h is the layer thickness, σ is the tensile stress in the y direction, and τ is the shear stress transmitted from the copper to the polyimide by the adhesive layer, given by

$$\tau(y) = \frac{\mu_A}{h_A}(v_P(y) - v_C(y)),$$

where v is the displacement field in the y direction, μ_A is the shear modulus of the adhesive, and h_A is the thickness of the adhesive layer. Using the strain-displacement relations and the plane-strain, elastic constitutive law (we take the displacement in the x direction to be zero) we find

$$\sigma_C(y) = \frac{E_C}{1-\nu_C^2} v'_C(y),$$
$$\sigma_P(y) = \frac{E_P}{1-\nu_P^2} v'_P(y),$$

where E is the Young's modulus, and ν is the Poisson's ratio.

Putting the above equations together and rewriting, the following system of linear, second order, ordinary differential equations is found

$$\begin{aligned} v''_P(y) &= \frac{-\mu_A(1-\nu_P^2)}{E_P h_A h_P}(v_C(y) - v_P(y)) \\ v''_C(y) &= \frac{2\mu_A(1-\nu_C^2)}{E_C h_A h_C}(v_C(y) - v_P(y)). \end{aligned} \tag{1}$$

The boundary conditions are that the displacement of the polyimide is zero at $y = 0$, the stress, σ_C, in the copper is zero at $y = 0$, the displacement in the polyimide and copper are equal away from the crack, and the stresses in the copper and polyimide away from the crack balance the applied load. In terms of the displacement fields, these boundary conditions are

$$\begin{aligned} &v_P(0) = 0, \\ &v_C'(0) = 0, \\ &v_C(\infty) = v_P(\infty), \\ &v_C'(\infty) = \sigma_C^\infty (1 - \nu_C^2)/E_C. \end{aligned} \tag{2}$$

The above equations were solved by converting the system of two second order equations into a system of four first order equations, which is then solved using the eigenvalue/eigenvector method. The result is

$$\begin{aligned} v_C(y) &= \frac{\sigma_C^\infty (1 - \nu_C^2)}{E_C} \left[\frac{\mathrm{e}^{-\lambda y}}{\lambda} + y + \frac{\omega}{\lambda} \right], \\ v_P(y) &= \frac{\sigma_C^\infty (1 - \nu_C^2)}{E_C} \left[\frac{-\omega\, \mathrm{e}^{-\lambda y}}{\lambda} + y + \frac{\omega}{\lambda} \right], \end{aligned} \tag{3}$$

where λ is the inverse of a characteristic decay length,

$$\lambda = \left[\frac{\mu_A}{h_A} \left(\frac{(1 - \nu_P^2)}{E_P h_P} + \frac{2(1 - \nu_C^2)}{E_C h_C} \right) \right]^{1/2},$$

ω is the ratio of the copper to polyimide stiffness,

$$\omega = \frac{E_C h_C (1 - \nu_P^2)}{2 E_P h_P (1 - \nu_C^2)},$$

and the far field tensile stress is

$$\sigma_C^\infty = \frac{Q}{h_C (1 + 1/\omega)},$$

where Q is the applied load per unit depth. Note that since the modulus of the polyimide is much less than the copper, away from the crack, most of the load is carried by the copper.

The effective spring constant, k, of the bridging layers is given by the ratio of the applied force to the displacement of the copper at the crack,

$$k = \frac{Q}{v_C(0)} = \frac{E_C h_C \lambda}{(1 - \nu_C^2)\omega} = \frac{2 h_P E_P \lambda}{(1 - \nu_P^2)}. \tag{4}$$

Having computed the bridging spring stiffness from a one-dimensional analysis, the stress intensity factor function can be estimated for our test specimen using the results of Rose (1987). Rose calculated the stress intensity factors for a finite crack in an infinite plate, bridged by linear springs. Although the test specimen is not an infinite plate, Rose's analysis is a good approximation when the crack size is small (as in the beginning of the tests).

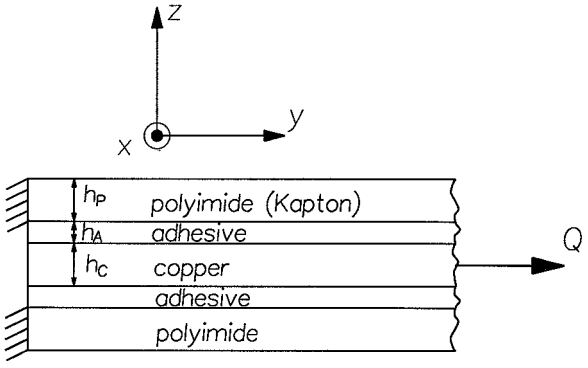

Figure 2. Layup of laminates, and geometry for shear lag model. View is of a cross section perpendicular to the crack line. Tensile stress in the laminate away from the crack is carried across the crack by the intact polyimide layer.

Having an analytical result reveals the scaling of the dependence of the crack shielding on the mechanical and geometric properties of the laminate which is important for design of the laminates against fatigue failure.

Rose showed that for a crack in an infinite plate under uniform far field stress the mode-I stress intensity factor is given by

$$K_{\mathrm{I}} = K_{\mathrm{I}}^{\text{no springs}} F_0, \tag{5}$$

where $K_{\mathrm{I}}^{\text{no springs}}$ is the stress intensity factor for a crack with no springs and K_{I} is the stress intensity factor for a crack bridged along its entire length by linear springs. For $\hat{k}a \gg 1$,

$$F_0 = \frac{1}{\sqrt{\pi \hat{k} a}}, \tag{6}$$

where $\hat{k}$ is the normalized spring constant, with units of 1/length,

$$\hat{k} = \frac{k}{E_C h_C} = \frac{\lambda}{(1-\nu_C^2)\omega}, \tag{7}$$

and a is the half crack length as defined in Figure 3.

The stress intensity factor, $K_{\mathrm{I}}^{\text{no springs}}$, is calculated using a known formula for a center cracked sheet [7],

$$K_{\mathrm{I}}^{\text{no springs}} = \frac{P}{2bh_C(1+1/\omega)}\sqrt{\pi a}(1 + 0.128(a/b) - 0.288(a/b)^2 + 1.525(a/b)^3), \tag{8}$$

where b is the sheet half width and P is the total applied load. The $(1+1/\omega)$ term accounts for the fraction of the far field load carried by the polyimide.

Putting the thicknesses and moduli into the above equations,

$$h_P = 50.8\,\mu m \Rightarrow \frac{1}{\hat{k}} = 1.8\,\mathrm{mm}, \qquad \frac{1}{\lambda} = 115\,\mu m, \quad \omega = 17.9,$$

$$h_P = 25.4\,\mu m \Rightarrow \frac{1}{\hat{k}} = 2.6\,\mathrm{mm}, \qquad \frac{1}{\lambda} = 83\,\mu m, \quad \omega = 35.9.$$

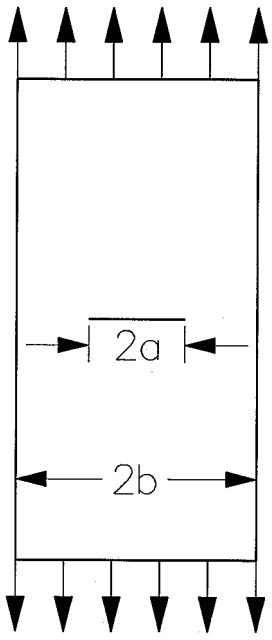

Figure 3. Center cracked test specimen. $2b = 50.8$ mm. Length $= 208$ mm.

The resulting stress intensity factor is shown in Figure 4. The degree of shielding, $1/F_0$, or the reduction in stress intensity for the same load due to the polyimide layers, is in the range of 5 to 11, depending on the crack length, and on polyimide thickness. Note that the length scale, $1/\lambda$, over which the shear stresses in the adhesive decay is approximately $3h_C$ for the given properties and thicknesses. The scaling of the reduction in K_{I} due to the bridging polyimide layers is

$$\frac{K_{\mathrm{I}}}{K_{\mathrm{I}}^{\text{no springs}}} \sim \left[\frac{E_C h_C}{\sqrt{E_P h_P}\sqrt{\mu_A/h_A}}\right]^{1/2} \sim \frac{(\text{copper stiffness})^{1/2}}{(\text{polyimide stiffness})^{1/4}(\text{adhesive stiffness})^{1/4}}. \tag{9}$$

Thus to maximize shielding, the stiffness of the polyimide and of the adhesive relative to the copper should be maximized within the design constraints.

3. Layered finite element analysis

The analytical calculation provides the scaling law for crack tip shielding and a good approximation of the stress intensity factor for short cracks. However, to analyze the experimental results the stress intensity factor for the laminates was needed over the full range of crack lengths. Thus finite element analyses were performed using FRANC2D/L (Swenson and James, 1996), an interactive program for the simulation of crack growth in layered structures such as lap joints. Each layer is represented using a separate mesh, that can be connected to the other layers by either adhesive or rivet elements. Each layer is assumed to be flat, but

either in-plane or bending calculations can be performed. Since there was no bending in these experiments, only the in-plane capability was used.

The elements used to represent in-plane behavior in each layer are standard eight or six noded serendipity elements with quadratic shape functions. These elements perform well for elastic analysis and have the advantage that the stress singularity at the crack tip can be incorporated in the solution by moving the side nodes to the quarter-point locations (Henshell and Shaw, 1975).

As in the analytic model, the adhesive elements transmit shear forces between layers. It is assumed that the adhesive layer is homogenous, linear elastic, and isotropic. The adhesive is assumed to deform only in shear and this deformation is uniform through the adhesive thickness. In the coordinate system of Figures 1 and 2, the shear stresses in the adhesive are given by

$$\begin{aligned} \tau_{xz}(x,y) &= \frac{\mu_A}{h_A}(u_P(x,y) - u_C(x,y)), \\ \tau_{yz}(x,y) &= \frac{\mu_A}{h_A}(v_P(x,y) - v_C(x,y)), \end{aligned} \tag{10}$$

where τ_{xz} and τ_{yz} are the shear stress components, u is the displacement in the x direction, and v is the displacement in the y direction. The adhesive forces on the layers are obtained by using the adhesive shear stresses as surface tractions and integrating. Since the surface tractions are proportional to the relative displacement of the two layers, the adhesive force can be expressed in terms of nodal displacements of the top and bottom layers. This gives a stiffness matrix for the adhesive elements.

Figure 5 shows the mesh used for the analysis. Symmetry was assumed along the left and lower edges, with a mesh 25.4 mm wide and 101.6 mm high (actual specimen size 50.8 mm by 203.2 mm). The crack length (a) in this mesh is 5.08 mm. Figure 5b shows a detail of the mesh near the crack tip. The elements along the crack line have a vertical (y) dimension of 0.102 mm. As the shear lag analysis shows, at the crack line the adhesive shear stresses decay over a distance of a few thicknesses. Thus, to capture this stress gradient the size of the elements along the crack line must be on the order of the adhesive layer thickness.

As mentioned above, the nodes of the elements surrounding the crack tip were moved to the quarter-points. This captures the stress singularity at the crack tip and allows accurate stress intensity calculations. For these analyses, the stress intensities were calculated using displacement correlation. Based on experience using this method, the calculated stress intensity factors are believed to be accurate within 5 percent. To verify this, a refined mesh case was calculated and it gave stress intensities within 2 percent of the present mesh.

The stress intensity factors as a function of crack length are shown in Figure 4 for both the finite element calculations and the analytical approximation. The key result is the dramatic reduction in stress intensity that results from the polyimide layer. A second notable feature is that the calculated stress intensities are approximately constant as the crack grows. For short crack lengths, the infinite sheet approximation used for the analytical calculation is valid, and the analytical results agree with the FEM results as expected.

The reason for the constant stress intensity factors is illustrated in Figure 6 which shows the crack opening displacement for a crack length of 5.08 mm. If the crack grew to the edge of the copper and completely broke the copper layer, the crack opening along the crack face would still be constant and finite due to the bridging of the polyimide. Figure 6 shows that the

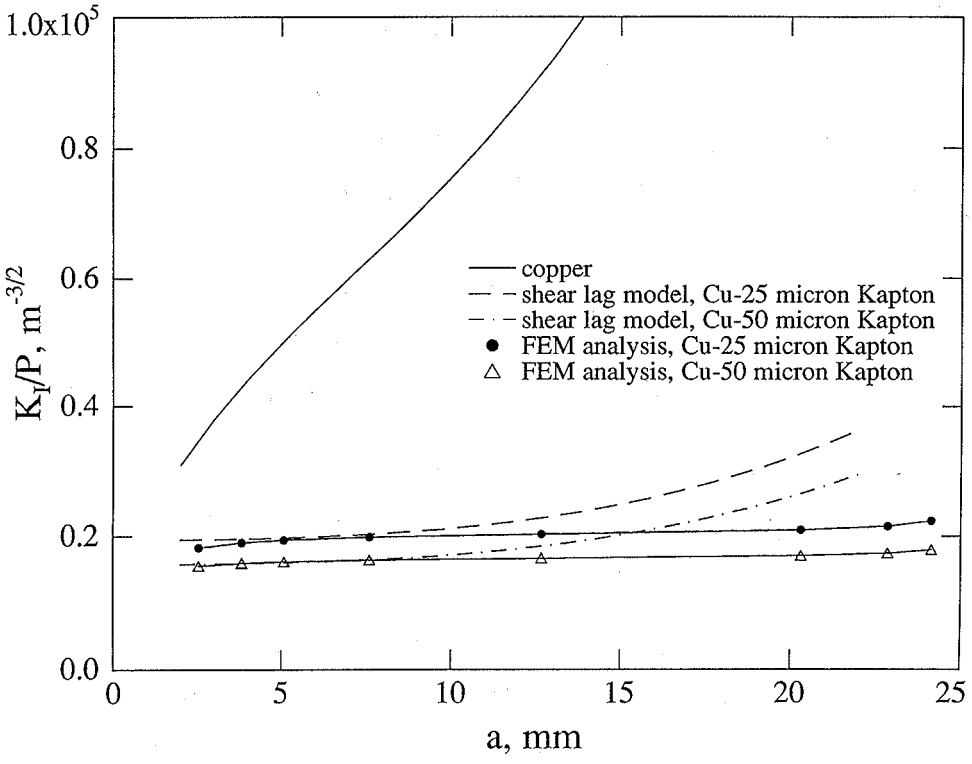

Figure 4. Stress intensity factor vs. crack length for the pure copper sample, and for the copper-polyimide samples analyzed using the shear lag and finite element models.

crack face opening does indeed approach this condition behind the crack tip. The consequence is that the stress intensity is approximately constant and independent of crack length.

Further details and confirmation of the results of the finite element calculation are given in Figure 7, which plots the shear stress, τ_{yz}, along a line normal to the crack face. The shear stress is normalized by its value at the crack face, and the distance is normalized by the thickness of the copper. To give an idea of the absolute value of the stresses, for $a = 5.1$ mm, $P = 111.2N$, (far field stress, $\sigma_C^\infty = 43$ MPa), at a distance of 1.3 mm behind the crack tip, $\tau_{yz}(0) = 7.9$ MPa. Also shown on Figure 7 is the normalized shear stress distribution predicted by the shear lag model. The finite element and shear lag model results agree almost exactly, which is to be expected since both approaches model the adhesive as a distributed shear spring, and sufficiently far behind the crack tip the stress state is essentially one-dimensional. Figure 7 also shows that the adhesive shear stress decays exponentially over a distance of approximately $10h_C$, (0.5 mm in this case) away from the crack line. Thus the transfer of load at the crack line from the copper to the polyimide occurs over a very small distance.

4. Experiments

4.1. Sample preparation

Pure copper and copper-polyimide(Kapton) laminates were tested using the center cracked sheet geometry shown in Figure 3. The pure copper samples were cut from rolled-annealed

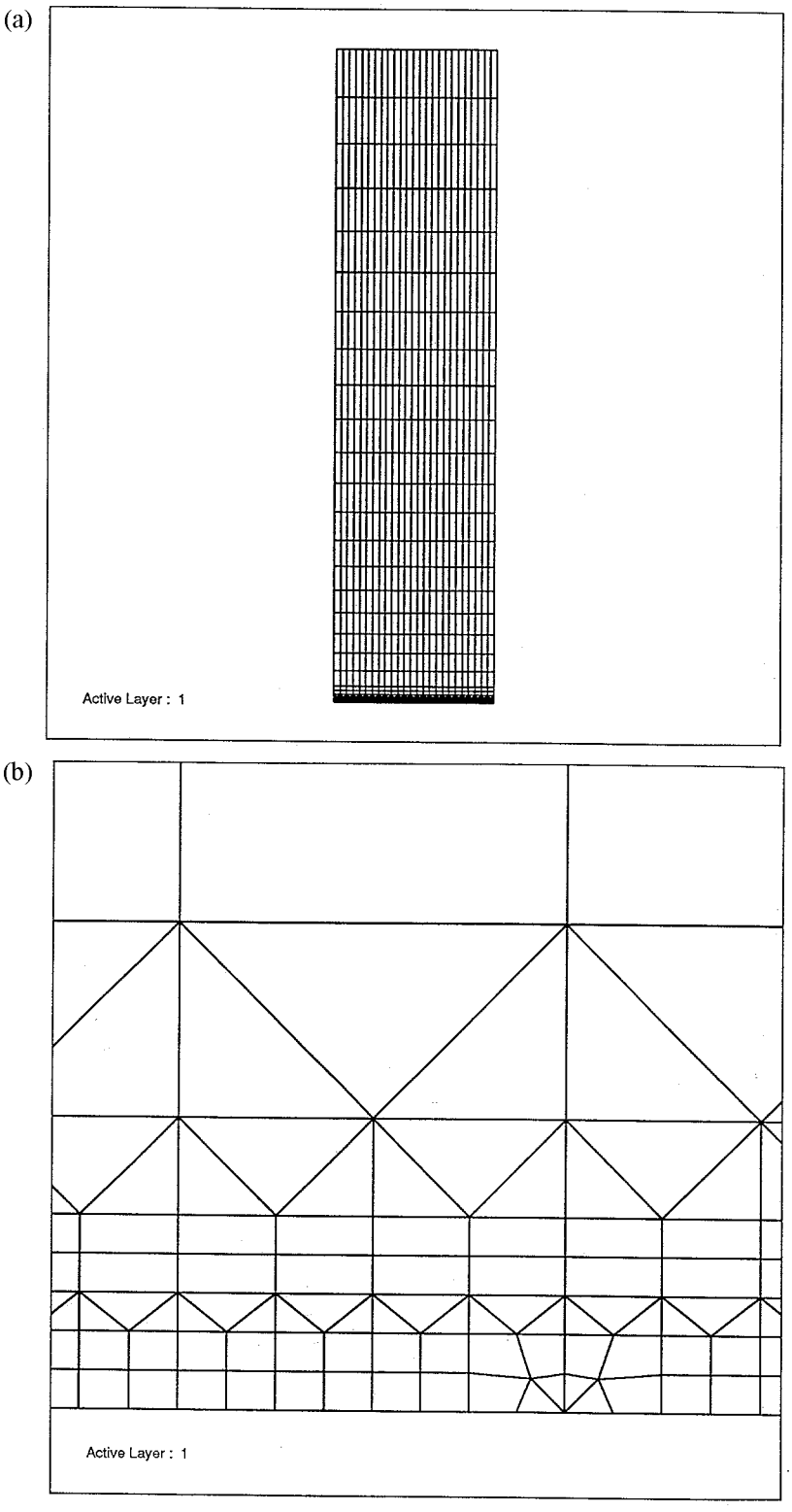

Figure 5. (a) Mesh used for layered finite element analysis. (b) Detail of the mesh near the crack tip.

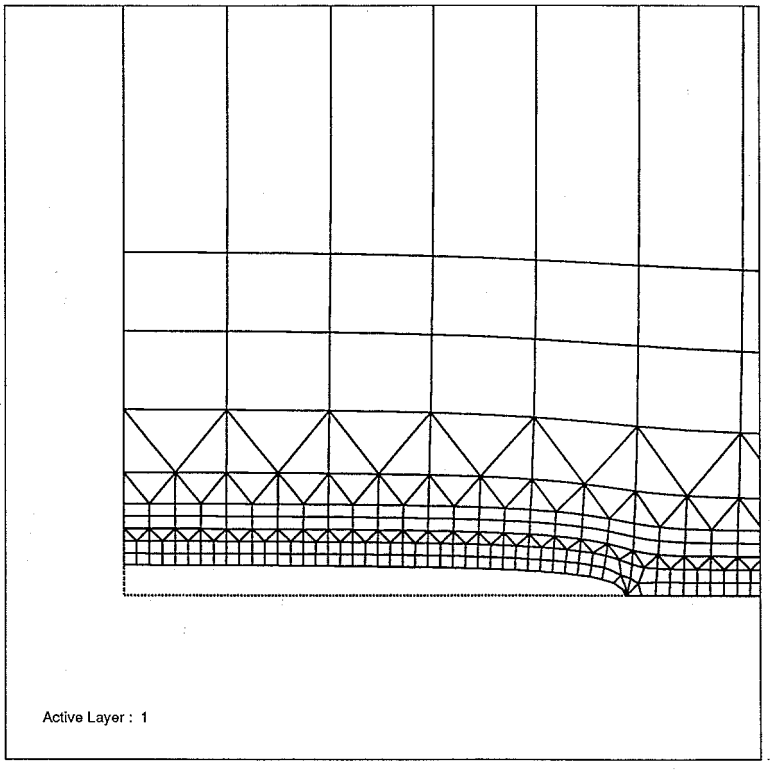

Figure 6. Crack opening displacement. Note that the polyimide bridging the crack keeps the crack opening displacement approximately constant.

copper sheet, 50 μm thick[1]. The laminated samples were made using 50 and 25 μm thick adhesive coated polyimide[2]. The samples were made by first cutting the copper to size, and cutting a precrack in the center of the copper using a square edge X-Acto knife. The polyimide layers were cut oversize, and the copper laminated between the upper and lower polyimide sheets. The laminate was placed in a hot press and heated in about 30 minutes to 190°C. Keeping the temperature at 190°C, a pressure of 1.4 to 2.8 MPa was then applied and held for 45 minutes. The sample was then allowed to cool under pressure in the hot press for 15 minutes before being removed. The excess polyimide was then trimmed from the specimen.

4.2. TEST SETUP

The samples were held between two rigid grips faced with 400 grit sandpaper. The grips themselves are loaded from their center as shown in Figure 8. All of the tests were performed using a 45,000 N capacity servo-hydraulic testing machine with a 4500 N capacity load cell. The tests were run at 5 to 20 Hz, with the ratio of minimum to maximum load, $R = 0.2$. Crack length was measured optically using a Questar long range microscope equipped with a traversing mechanism and a dial gauge to measure its position. Crack length measurements were performed approximately every 0.5 mm of crack growth. For analysis, the crack length

[1] Lyon Industries.
[2] DuPont Pyralux LF0120 and LF0110.

Table 2. Summary of tests

Test #	Material	ΔP, N	f, Hz	Cycles to reach $a = 12.7$ mm
C1	copper	112	20	479 000
C2	copper	112	20	643 000
CK1	copper-50 μm polyimide	534	20	274 000
CK2	copper-50 μm polyimide	534	20	353 000
CK3	copper-50 μm polyimide	800	5	14 200
CK5	copper-50 μm polyimide	445	10	675 000
CK6	copper-25 μm polyimide	445	10	234 000

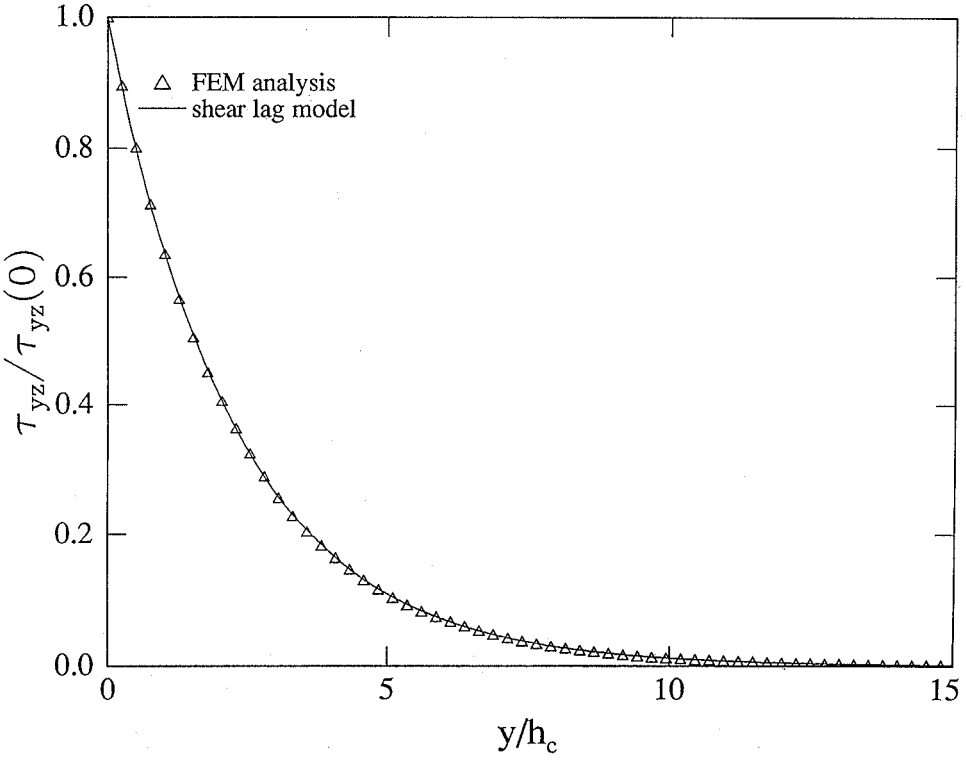

Figure 7. Shear stress distribution normal to the crack line. Results are for 50.8 μm thick polyimide.

used is the average crack length, i.e. one-half of the sum of the initial crack length and the growth of the left and right cracks. In some tests one crack grew much faster than the other. Data from such tests were disregarded. The crack length data is differentiated using the incremental polynomial fit method[3], where a quadratic equation is fit to 5 points, two on either side of the point at which growth rate is desired. The tests that were run and that were analyzed are summarized in Table 2.

[3] See ASTM standard E-647.

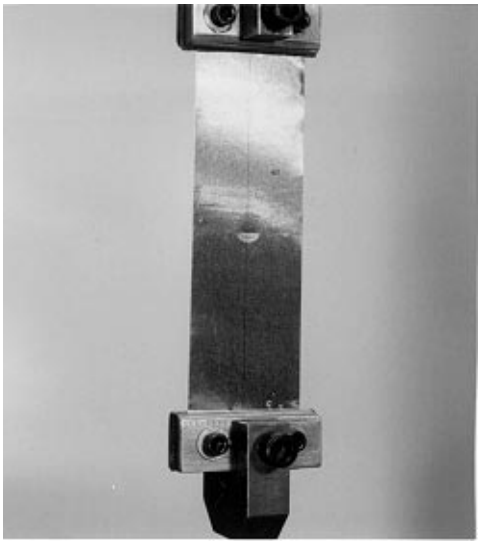

Figure 8. Photograph of test specimen and grips in testing machine.

4.3. RESULTS

Figure 9 shows the crack length history for a copper sample loaded at $\Delta P = 112N$, and for a copper-50 μm polyimide sample loaded at $445N$. The plot shows that the crack growth rate is approximately the same for these two tests. That is, to achieve the same crack growth rate in the laminate as in the pure copper, the load must be four times larger, which is in the same range as the predicted degree of shielding.

The crack growth rate in the copper sample increased continuously, as expected, since for constant amplitude loading, K_{I}, given by Equation (8) increases sharply with crack length. The data from the pure copper tests was analyzed using Equation (8) (with $1/\omega = 0$). The resulting fatigue crack growth rate for two tests on pure copper is shown in Figure 10, along with a log-log fit to the data,

$$\log_{10} \mathrm{d}a/\mathrm{d}N = -33.5 + 3.81 \log_{10} \Delta K_{\mathrm{I}}, \tag{11}$$

where $\mathrm{d}a/\mathrm{d}N$ is in m/cycle and ΔK_{I} is in $N/m^{3/2}$. Note that the variation in ΔK and hence in $\mathrm{d}a/\mathrm{d}N$ for the copper samples is sufficient to cover one decade in crack growth rate from a single load amplitude.

Figure 9 shows that the growth rate for the copper-polyimide samples is close to being constant. This result, puzzling at first, is explained by the results of the layered FEM analysis, Figures 4 and 6. The stress intensity factor and crack opening displacement in the laminates is essentially constant with crack growth. As the crack advances the polyimide bridging the crack carries an increasing amount of the load unlike the pure copper case where the load must be carried by an ever shrinking remaining uncracked ligament. Note that for a finite crack in an infinite plate, Rose's analysis also predicts constant stress intensity factor. Since K_{I} and hence $\mathrm{d}a/\mathrm{d}N$ are essentially constant, for the laminates, several tests at different loads were performed to find the variation of $\mathrm{d}a/\mathrm{d}N$ vs. ΔK_{I}.

The results of these tests were analyzed using the stress intensity factors computed by the layered FEM analysis, plotted in Figure 4. The crack growth rate vs. the stress intensity factor

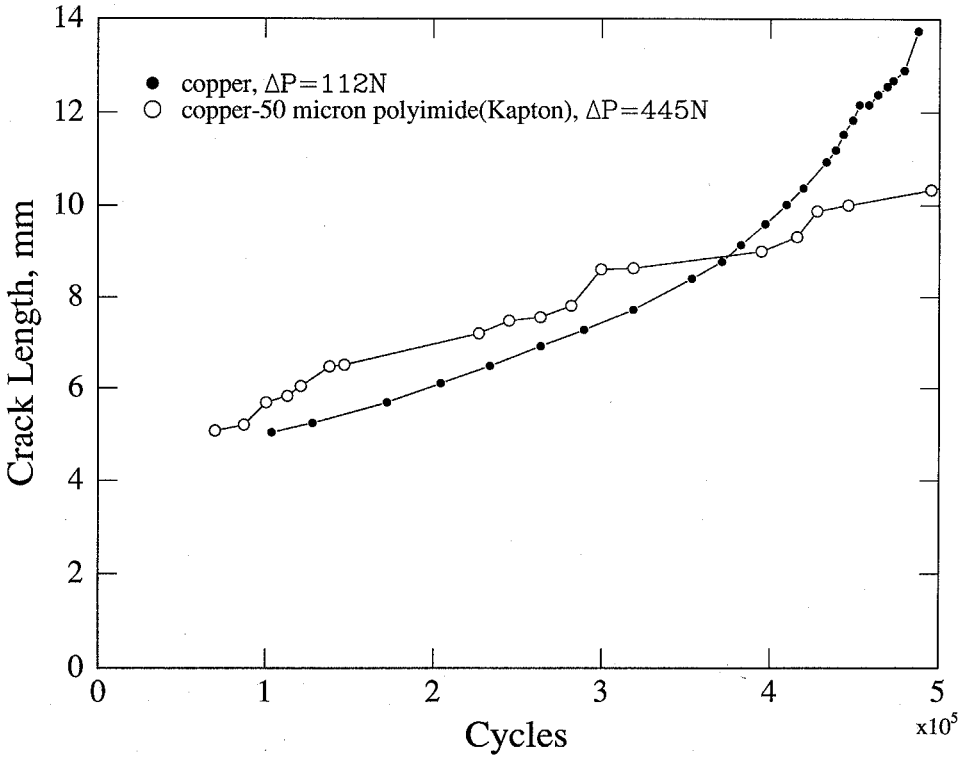

Figure 9. Crack length record for a pure copper sample loaded at $\Delta P = 112N$, and for a copper-polyimide sample loaded with $\Delta P = 445N$.

(calculated taking into account the shielding of the polyimide) is on the plot of Figure 10. It can be seen that the crack growth rate from the copper-polyimide laminates correlates well with the data for pure copper. If we postulate that crack growth rate is governed solely by the stress intensity factor of the copper, the correlation of the copper-polyimide and copper data show that indeed the polyimide is shielding the crack tip and that the degree of shielding is closely approximated by the results of the analyses. That the crack growth rate for the laminates is somewhat lower than the pure copper suggests that the analyses underpredict the amount of shielding that occurs, or that the processing of the laminates and the presence of the polyimide change the environment of the copper in a way that slows the crack growth rate.

4.4. Effect of polyimide thickness

The scaling given by Equation (9) suggests that for the same load, in the thinner polyimide (one-half the thickness of the thicker) the stress intensity factor will be $2^{1/4} = 1.2$ times larger than in the thicker polyimide. From the crack growth rate correlation for the copper, Equation (11) this should result in an average crack growth rate $(1.2)^{3.8} \approx 2$ times faster in the thin laminate than the thick laminate. The crack length records for a thick and a thin laminate sample, both loaded at $\Delta P = 445N$ are shown in Figure 11. This plot shows that the average crack growth rate for the thin laminate was approximately 2.6 times faster than the average rate for the thicker laminate. Although this is a somewhat larger difference than

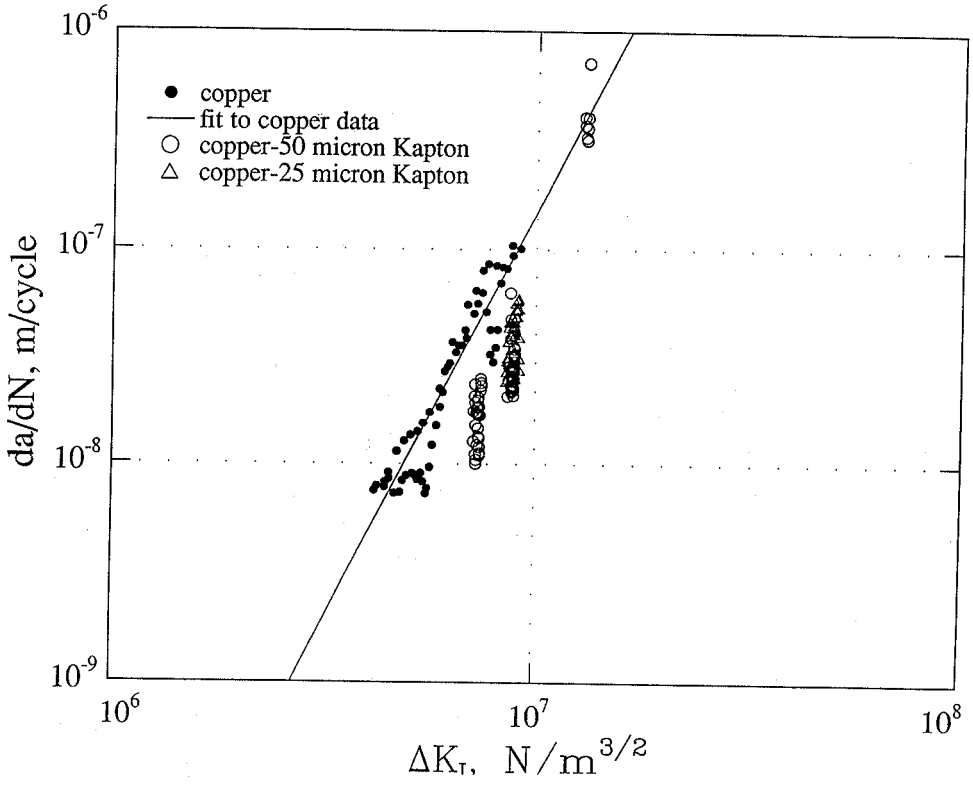

Figure 10. Fatigue crack growth rate for copper and copper-polyimide samples, $R = 0.2$. Note that although the copper-polyimide data fall close to the copper data, the loads for the copper-polyimide samples were much higher that for the copper samples. The stress intensity factors, however, are approximately the same due to the large amount of crack tip shielding provided by the polyimide.

predicted, it shows that the analysis is essentially correct in predicting the scaling and trends of crack growth.

5. Discussion

The data of Figure 10 show that the crack growth rate for the copper-polyimide laminates lies somewhat below that for pure copper. This could be due, in part, to residual stresses and in part to the contribution of the adhesive layer to the laminate stiffness.

In the copper-polyimide laminates, the thermal expansion coefficient, α of the polyimide (see Table 1) is slightly larger than copper, resulting in a small compressive residual stress in the copper, which would reduce the crack growth rate somewhat. However, if one assumes the usual force equilibrium and strain compatability, the magnitude of the residual compressive stress in the copper is only 6 MPa. Typical nominal stresses applied in the experiments were in the range of 100–200 MPa, thus the residual stress is small relative to the applied stress and will have a very small effect on the crack growth rate.

It was assumed that the adhesive layer carries no tensile load, only interlayer shear stresses. However, the stiffness of the adhesive layer is non-zero and does carry some load in the far field, which slightly reduces the crack tip stresses. However, since it is assumed that the

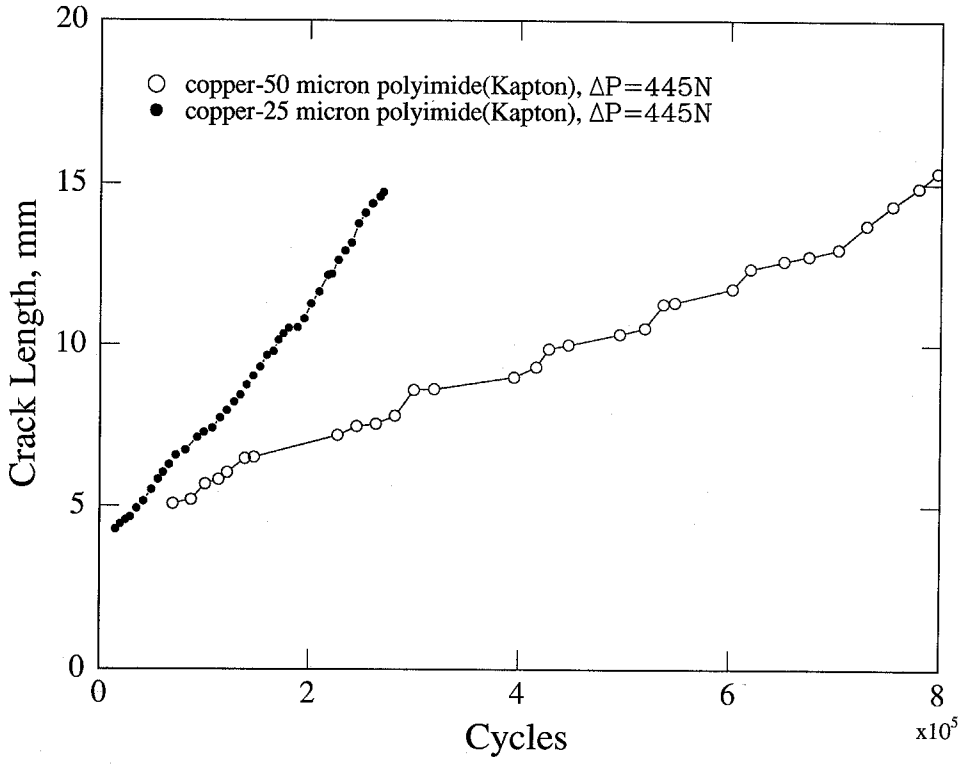

Figure 11. Crack length record for laminates with 25 μm and a 50 μm polyimide. Both tests were run at $\Delta P = 445N$. The rate of crack growth in the 25 μm polyimide laminate is approximately three times faster than in the 50 μm laminate.

adhesive is cracked through, it cannot contribute to the bridging, which is the most important factor in shielding the crack.

Fatigue crack growth is known to be rate dependent due to environmental effects. The experiments were all run in a narrow frequency range, 5–20 Hz. In such a narrow range it is expected that the rate effects would be essentially the same in all of the experiments, and hence not be a factor in the differing crack growth rates.

One may question the applicability of linear elastic fracture mechanics (LEFM) to fatigue in a ductile metal such as copper. One way to determine if LEFM is valid is to estimate the plastic zone size, approximated for plane stress by [10]

$$r_p = \frac{1}{\pi}\left(\frac{K_{\mathrm{I}}}{\sigma_0}\right)^2,$$

where r_p is the plastic zone size, and σ_0 is the yield stress. The maximum value of K_{I} was approximately 13 MPa $\sqrt{\mathrm{m}}$, and the yield stress (measured in our lab by tensile testing) is approximately 180 MPa, resulting in a *maximum* plastic zone size of $r_p = 1.7$ mm, which is small (6 percent of b) relative to the in-plane dimensions of the test specimen. Thus, except perhaps at the final stages of crack growth, small scale yielding conditions prevail and the application of LEFM to correlate the data is justified.

The experimental results and the analyses show that for the materials considered here the plastic layers provide substantial shielding of the crack tip and hence enhanced fatigue life.

Whether this is a more general phenomenon is not known, but we suspect that it is, i.e. polymer layers can provide substantial crack tip shielding despite their low elastic modulus relative to the metal. The requirements for effective shielding are that the polymer layer itself is tough so that it does not crack, that the bond between the metal and polymer layers is sufficiently strong to prevent significant debonding, which would reduce the bridging stiffness, and that the adhesive layer is thin, increasing its shear stiffness and hence the bridging stiffness.

Reinforcement of metals with polymers obviously has it limits, since the polymer layers will not be able to sustain infinite loads or may debond from the metal at high loads. This was found in the experiments. When we attempted to increase the load applied to a copper-25 μm polyimide laminate beyond 1000N, the sample delaminated and fractured immediately. At this load the applied stress is approximately 380 MPa, well over the copper's yield stress, resulting in unconstrained plastic flow of the copper, leading to delamination and overall failure.

6. Summary and conclusions

Polyimide layers of approximately the same thickness as a copper layer bridge across cracks in the copper effectively shielding the copper and allowing a copper-polyimide laminate to bear approximately four times the load of a pure copper sample for the same fatigue life. That the polymer can reinforce the metal despite the low elastic modulus of the polymer is a result of the thin and tough adhesive layer between the polymer and the metal, which renders the effective length of the polymer bridging the crack to be small, resulting in a stiff spring across the crack. This conclusion is supported by experiments, analytical approximations, and layered finite element analyses. Results from the layered finite element analysis agree closely with the shear lag analysis for short crack lengths verifying the accuracy of the layered finite element method computations. The scaling laws for the crack shielding are calculated based on a shear lag model.

Acknowledgements

The experimental work was supported by the National Science Foundation through a Research Experience for Undergraduates grant to Cornell, EEC-9300579. Development of the layered finite element method was supported by NASA Langley, through NAG-1-1503 to Kansas State University. The experiments were performed using the Mechanical Testing Facility of the Materials Science Center at Cornell, funded by the NSF under award DMR-9121654. The authors would like to thank Dr. Mark Viz, Mr. George Chevalier and Ms. Eve Pienkos for their assistance with the experiments, Mr. Mark James for major development of FRANC2D/L, and Prof. Anthony Ingraffea for discussing this work with us.

References

Hellan, K. (1984). *Introduction to Fracture Mechanics*, McGraw-Hill, New York, 18.

Henshell, R.D. and Shaw, K.G. (1975). Crack tip finite elements are unnecessary. *International Journal for Numerical Methods in Engineering* **12**, 93–99.

Rose, L.R.F. (1981). An application of the inclusions analogy for bonded reinforcements. *International Journal of Solids and Structures* **17**, 827–838.

Rose, L.R.F. (1987). Crack reinforcement by distributed springs. *Journal of the Mechanics and Physics of Solids* **35**, 383–405.

Schive, J. (1991). Predictions on fatigue. *JSME International Journal, Series I* **34**, 269–280.

Swenson, D. and James, M. (1996). FRANC2D/L: A crack propagation simulator for plane layered structures – Version 1.2 User's Guide. Kansas State University, Manhattan, Kansas, 66506.

Tada, H., Paris, P. and Irwin, G. (1985). *The Stress Analysis of Cracks Handbook*, Del Research Corporation, St. Louis.

Tarn, J.-Q. and Shek, K.-L. (1991). Analysis of cracked plates with a bonded patch. *Engineering Fracture Mechanics* **40**, 1055–1065.

Yeh, J.R. (1995). Fatigue crack growth in fiber-metal laminates. *International Journal of Solids and Structures* **32**, 2063–2075.

Zehnder, A.T. and Ingraffea, A.R. (1995). Reinforcing effect of coverlayers on the fatigue life of copper-polyimide flex cables. *IEEE Transactions on Components, Packaging, and Manufacturing Technology – Part B: Advanced Packaging* **18**, 704–708.